4^{th} URSI AT-RASC, Gran Canaria, 19 – 24 May 2024

Polarisation Insensitive Active FSS for EM Shielding

Saikiran Kongari[(1)],Anand Kumar[(1)],Yugesh Chandrakapure [(1)], and Debdeep Sarkar[(1)]
(1) Dept. of ECE, Indian Institute of Science, Bengaluru-560012, Karnataka, India.
e-mail: anandkumar13@iisc.ac.in

Abstract

This paper proposes a narrowband polarisation insensitive transmissive/reflective frequency selective surface (FSS). The FSS comprises unit cells with square and circular metallic loops connected by PIN diodes controlled by a biasing source. In contrast to typical wideband FSSs, the structure provides 0.55 GHz of narrow stopband (a fractional bandwidth of 22%) at 2 GHz in the OFF state bias. The bandstop response can be adjusted by varying the reverse bias voltage. The FSS alternates between its functionalities and, in forward bias, provides a passband at the operational frequency. The structure is compact and operates as a transmissive/reflective surface under two different bias conditions (ON and OFF). The design is angularly stable and polarization-insensitive for both TE and TM polarisation. A prototype of the designed structure is developed and the measured results correlate well with the simulated responses.

1 Introduction

With the fast growth in wireless technology, the issue of electromagnetic interference (EMI) among neighboring electronic gadgets and electrical machinery in sensitive surroundings has been emerging [1]. A frequency selective surface (FSS) can be used to shield such devices and is an excellent solution for many applications because of its low cost, small profile, and ease of production. Furthermore, FSSs can provide band-pass or band-stop responses and are frequently used in microwave and millimeter-wave regimes as spatial filters, antenna reflectors, radomes, absorbers, artificial magnetic conductors, etc [2]. Interference reduction and security improvement among the neighboring wireless local area networks (WLAN) have been the focus of extensive research in recent years [3, 4, 5].

Active FSS, which can function as tunable or switchable FSSs using active components, have been recently explored [6, 7, 8]. The frequency response of these FSSs can be varied by biasing the active devices incorporated in their periodic arrays, as active devices enable high-speed and band tuning in a compact and low-cost package. The FSS structure reported in [6] can offer various functions but is polarization-sensitive. While in [7], a polarization-insensitive FSS with multiple layers is reported only for absorbing the EM waves but not for transmissive function. In [8], the structure provides frequency tuning, polarization selection, and electromagnetic switching in a single design; however, it requires two layers of active components with a diode for each operation. Varactor-driven adjustable structures have recently become popular, offering EM shielding and polarization-insensitive property [9, 10]. The structure in [9] is complicated as it calls for layer modifications based on operation, whereas the structure reported in [10] is solely addressed for its shielding behavior and does not discuss the transmissive nature. Therefore, it is necessary to develop a single structure with less complexity to achieve multiple functions such as various states (transmissive + reflective) as well as polarisation insensitivity.

In this paper, the authors have aimed to address some of the above-mentioned limitations by developing an FSS that can offer different functionalities based on its bias state. Although the proposed structure's design is inspired by the work presented in [10], wherein the unit cell has been modified by replacing the varactor diodes with the PIN diodes, the proposed design offers improved functionalities and additional features. The proposed FSS has been fabricated and tested successfully. The designed structure can offer the following features:

- The proposed FSS is simple in its design to offer multiple functionalities without complexity.
- The structure can function as a switchable transmission/reflection surface at a tunable frequency under different reverse bias voltages.
- It can offer more than 30 dB attenuation over a narrowband of 0.55 GHz (22 % bandwidth).
- The design exhibits fourfold symmetry, providing tunable characteristics for all polarization angles.

The format of the paper is as follows. The proposed structure's design is explained in Section II. The parametric analysis and simulations are presented in Section III. Section IV covers The fabricated prototype and its measurements' findings. Lastly, the final section contains the conclusion.

2 FSS Structure Design

Fig. 1 shows the array and unit cell design of the proposed FSS. Metallic square and circular loops are printed in a periodic manner on the dielectric substrate, and semiconductor switches (PIN diodes) are diagonally placed between the square and circular loops. The substrate used is FR4, with a relative permittivity (ε_r) of 4.4 and a loss tangent (tanδ) of 0.02. The top metallic patch is made up of copper, with a conductivity of 5.8×10^7 S/m and a thickness of 0.035 mm. The incident field directions are also shown in Fig. 1.

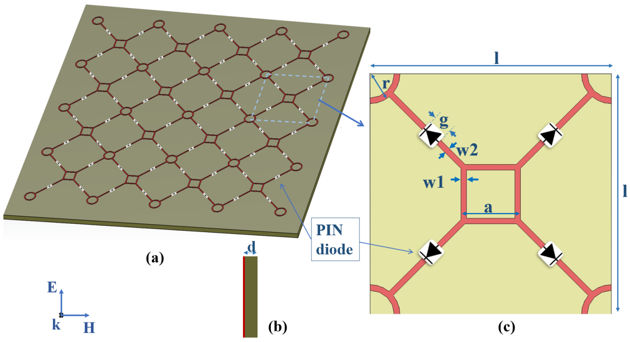

Figure 1. Schematic diagram of the proposed switchable FSS prototype. (a) Perspective view of the FSS. (b) Side view, and (c) top view of the unit cell. The dimensions of the optimally designed unit cell are: l = 54, a = 11, r = 5.5, w1 = w2 = 1.2, g = 2 and t = 1. (All dimensions are in mm.)

The operating frequency can be controlled by varying the cell size (l = 54 mm, inter-spacing between the loops) and the sizes of the loops (a and r). It is known that the frequency (λ_g) of reflection or absorption by an FSS relies on the perimeter of patch loops in such a way that λ_g is $2\pi r$ (or $4a$), where r is the radius of the circular loop and a is the side of the square loop. Initially, an air gap between the loops provides a lower capacitance, making the structure operate at a higher frequency. The capacitance in these gaps can be modified by incorporating PIN diodes, whose capacitance is higher than that of air. Here, the working frequency shifts in accordance with the bias voltage. Therefore, by optimizing the aforementioned unit cell parameters, the operating frequency of 2 GHz is attained.

The designed structure is intended to function as a transmissive/reflective surface at 2 GHz. The switches employed are the BAP64-03 Silicon PIN diodes [11], from NXP Semiconductors, that can operate up to 3 GHz, and our operating frequency is 2 GHz. When a reverse bias is applied, the operating frequency band can shift between 2 to 3 GHz range (1 GHz tuning bandwidth). So, to enhance this tuning bandwidth above 1 GHz, we can redesign this structure at a frequency lower than 2 GHz. These diodes possess variable capacitance and resistance under reverse and forward voltages. The intrinsic layer's depletion region expands with increased reverse bias on the PIN diode, decreasing capacitance. As a result, the frequency of operation increases.

3 Simulated Results and Parametric Analysis

The unit cell is modeled using periodic boundary conditions in the CST Microwave Studio. The following subsections provide more details on the different simulation results that are obtained.

3.1 FSS in the OFF state

Firstly, the structure is simulated in the PIN diode's OFF state, i.e., at '0 volt' of biasing. The diode offers a capacitance of 0.147 pF, which is observed through characterization. The transmission ($|S_{21}|$) & reflection ($|S_{11}|$) coefficients are shown in Fig. 2. As observed, the structure provides a narrow stopband of 0.55 GHz that is 22.22% w.r.t.

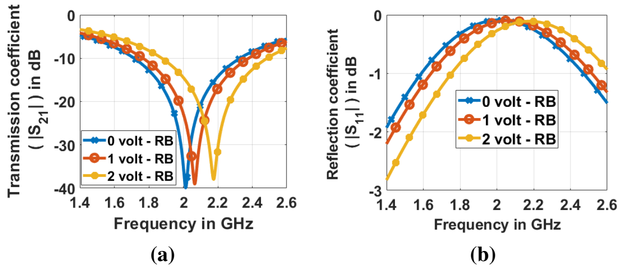

Figure 2. Simulated (a) transmission and (b) reflection coefficients of the structure in the OFF state.

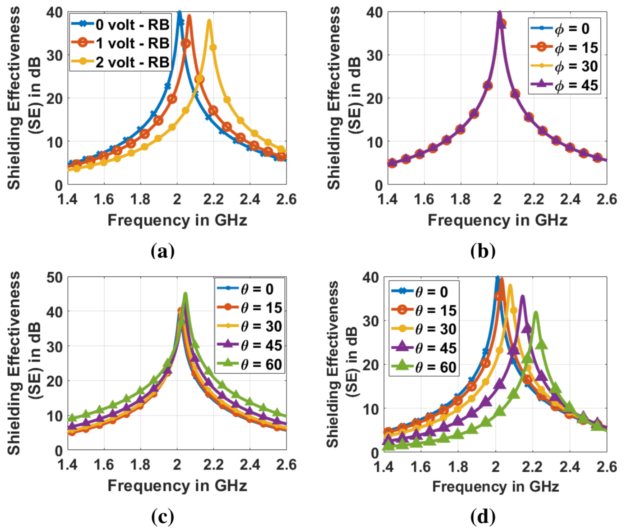

Figure 3. Simulated Shielding Effectiveness (SE) of the FSS for (a) various bias states, (b) different polarization angles ϕ under normal incidence, (c) different incident angles θ under TE polarization, and (d) different incident angles θ under TM polarization.

center frequency with a -10 dB attenuation level for all applied reverse voltages. $|S_{21}|$ is observed to be nearly -40 dB at the operating frequency. As mentioned earlier, this frequency is tunable by varying the reverse bias voltage. The structure's resonance can be explained in the way that follows. The EM wave striking the FSS's metal layer induces a surface current to flow, creating an equivalent inductance. The diode also contributes inductance and capacitance, collectively providing the resonance [2]. Tuning of the structure can be done by altering the capacitance offered by the diode w.r.t. the reverse bias. As observed in Fig. 2a, the resonance frequency shifts from 2 to 2.2 GHz as the reverse voltage increases from 0 to 2 V.

Shielding effectiveness (SE) is defined as the ratio of the transmitted field component (E_t) to the incident field component (E_i). It can address the shielding performance of an FSS and is represented by [1]:

$$SE_{dB} = -20 \times \log\left(\frac{E_t}{E_i}\right) \tag{1}$$

The SE of the proposed structure is shown in Fig. 3a and demonstrates an SE much higher than 30 dB for all the reverse bias voltage. The structure has a fourfold symmetrical design that makes it polarization insensitive, i.e., equal SE performance for all polarisation angles as shown

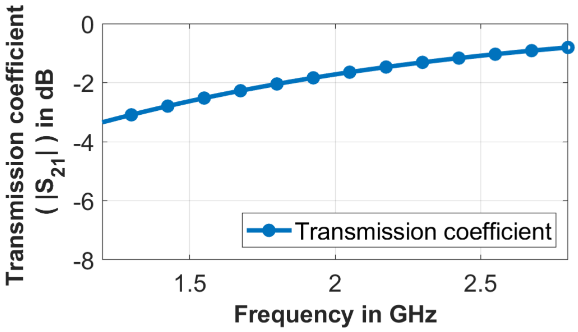

Figure 4. Simulated transmission coefficient of the switchable FSS in the ON states

in Fig. 3b. The structure has been further examined for various oblique incidences for different polarizations. Figs. 3c and 3d demonstrate the SE performance for the TE and TM polarizations of the incident wave, respectively. It can be noticed that a consistent stopband responses up to 60° angle of incidence.

3.2 FSS in the ON state

The structure is also simulated for the case of the PIN diode's ON state, i.e., at '1 volt' of biasing. The diode has a resistance of 20 Ω as measured by characterization. The diode can function as a variable resistor with a resistance inversely proportional to the forward bias voltage. In Fig. 4, the corresponding transmission coefficient ($|S_{21}|$) is presented and achieves a transmission of about -1.8 dB at the operating frequency of 2 GHz.

4 Prototype Fabrication and Measured Results

The proposed FSS, as stated in Section II, is fabricated and tested. DC bias lines are introduced in the structure to control the bias states of PIN diodes, as shown in Fig. 5. The fabricated prototype has physical dimensions of 290 mm × 275 mm, which consists of 4 × 4 arrays of unit cells. The measurement result shows that the structure operates at 2 GHz, with slight deviations from the simulated results, which can be accounted for by fabrication tolerance.

The circular loops of the unit cell are connected to the left-side bias line, while square loops are connected to the right-side bias line. The anode and cathode of the diodes are connected to the right and left bias lines, respectively. Murata Electronics LQG18HH10NJ00D inductors with 10 nH values are used in consecutive central square loops to achieve isolation and protect the biasing lines from EM interference. Bias lines allow direct current to flow continuously through PIN diodes.

The measurement setup is shown in Fig. 6. It is organized by placing the testing structure between the two Vivaldi antennas facing each other. The FSS is kept at the far field distance from the Tx antenna. Both antennas are connected to the Vector Network Analyzer to estimate the structure's reflection/transmission coefficient. At 2 GHz, when there

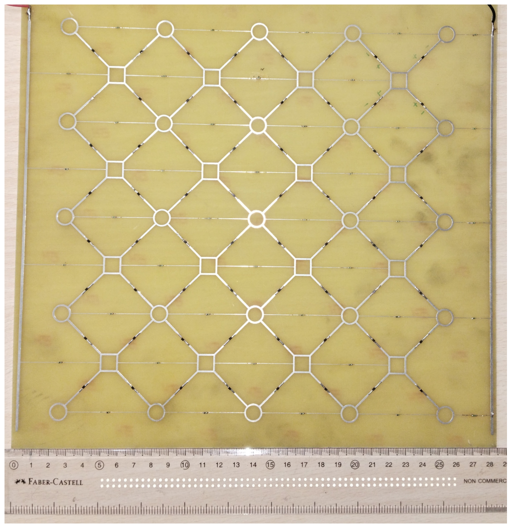

Figure 5. Fabricated prototype of the FSS

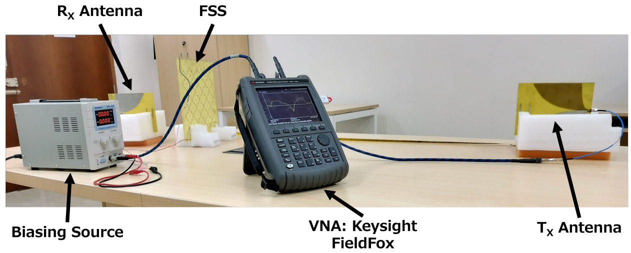

Figure 6. S-parameter Measurement setup for the FSS.

is no obstruction between the antennas, the power transmitted between the antennas is -31 dB, which is close to the calculated value using the Friis' transmission equation.

The transmission coefficients ($|S_{21}|$) are measured between the antenna system in the subsequent steps under various configurations of the FSS. As shown in 7, $|S_{21}|$ is initially measured in the OFF state and is observed to be at -62 dB at the operating frequency. It should be noted that the attenuation level is about 30 dB, which is in agreement with the simulated results. The shielding performance can be tuned by varying the reverse bias voltage. From Fig. 7, the change

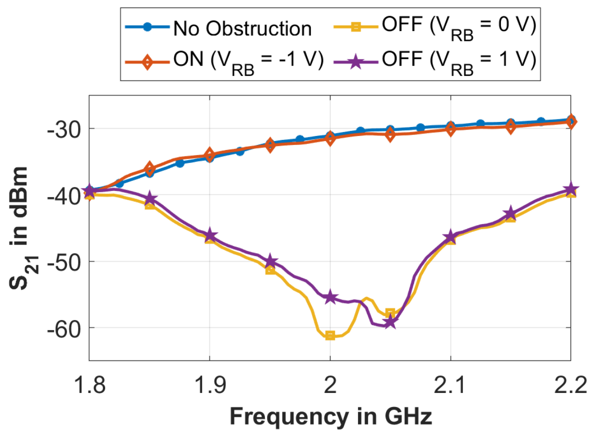

Figure 7. Measurement of Transmission coefficient for the proposed structure under different configurations

in shielding resonance to 2.06 GHz can be observed for 1 volt. Therefore, the structure is best suited for shielding applications in the open air at and around 2 GHz.

The FSS's ON state performance is measured by forward biasing the structure. In Fig. 7, the transmission coefficient is observed to be -33 dB. Observing an attenuation of nearly 2 dB, which is again close to the simulated results. Therefore, the proposed structure functions as a good tunable and switching FSS at 2 GHz. Fabrication tolerances, parasitic capacitance, and inductance effects of PIN diodes account for the minor measurement discrepancies.

5 Conclusion

This work proposes an active FSS with a tuneable narrowband reflective/transmissive response. The proposed FSS prototype is fabricated and tested. The simulation and measurement results show that the FSS has a switchable performance between nearly transparent and better shielding. Furthermore, the reported structure demonstrated a narrowband shielding with of about 0.55 GHz in the vicinity of 2 GHz. The suggested structure can also provide a wide tuning range for similar bandstop responsiveness as a function of reverse bias voltage as measured with the prototype. Furthermore, the structure has the advantages of less complexity in geometry, polarisation insensitivity, and angular stability by obtaining a significant degree of agreement between simulation and experimental results.

Acknowledgements

Aspects of the work have been funded by SERB, Dept. of Science & Technology, Government of India (GoI), through grant no. SRG/2021/000831 and PMRF, Ministry of Education, GoI, through grant no. TF/PMRF-22-3965.

References

[1] S. Celozzi, R. Araneo, P. Burghignoli, and G. Lovat, *Electromagnetic Shielding: Theory and Applications*, John Wiley & Sons, 2023.

[2] B. A. Munk, *Frequency selective surfaces: theory and design*, John Wiley & Sons, 2005.

[3] U. Farooq et al., "Ultraminiaturised polarisation selective surface (pss) for dual-band Wi-Fi and WLAN shielding applications," *IET Microwaves, Antennas & Propagation*, **14**, 13, 2020, pp. 1514–1521.

[4] C. Chattopadhyay, S. Coomar, S. Mondal, and R. Sanyal, "Highly selective, fractal-configured UWB-FSS for sub-6 GHz 5g, GSM, WLAN, and C band electromagnetic stealth application," *International Journal of Microwave and Wireless Technologies*, 2023, pp. 1–14.

[5] U. Farooq, M. F. Shafique, A. Iftikhar, and M. J. Mughal, "Polarization-insensitive triband FSS for RF shielding at normal and higher temperatures by retrofitting on ordinary glass windows," *IEEE Transactions on Antennas and Propagation*, **71**, 4, 2023, pp. 3164–3171.

[6] R. Phon, S. Ghosh, and S. Lim, "Novel multifunctional reconfigurable active frequency selective surface," *IEEE Transactions on Antennas and Propagation*, **67**, 3, 2018, pp. 1709–1718.

[7] C. Huang, J. Song, C. Ji, J. Yang, and X. Luo, "Simultaneous control of absorbing frequency and amplitude using graphene capacitor and active frequency-selective surface," *IEEE Transactions on Antennas and Propagation*, **69**, 3, 2020, pp. 1793–1798.

[8] H. Li, Q. Cao, L. Liu, and Y. Wang, "An improved multifunctional active frequency selective surface," *IEEE Transactions on Antennas and Propagation*, **66**, 4, 2018, pp. 1854–1862.

[9] X. Zeng, M. Gao, L. Zhang, G. Wan, and B. Hu, "Design of a tuneable and broadband absorber using a switchable transmissive/reflective FSS," *IET Microwaves, Antennas & Propagation*, **12**, 7, 2018, pp. 1211–215.

[10] S. Ghosh and K. V. Srivastava, "Broadband polarization-insensitive tunable frequency selective surface for wideband shielding," *IEEE Transactions on Electromagnetic Compatibility*, **60**, 1, 2017, pp. 166–172.

[11] N. Semiconductors, *BAP64-03 Silicon PIN Diode*, Product data sheet, Rev. 9—11 March 2019.